# Long Short-Term Memory Recurrent Neural Network Approach for Approximating Roots (Eigen Values) of Transcendental Equation of Cantilever Beam

Madiha Bukhsh [1,*], Muhammad Saqib Ali [2], Abdullah Alourani [3], Khlood Shinan [4], Muhammad Usman Ashraf [5], Abdul Jabbar [6] and Weiqiu Chen [1,*]

1 Key Laboratory of Soft Machines and Smart Devices of Zhejiang Province, Department of Engineering Mechanics, Zhejiang University, Hangzhou 310027, China
2 College of Electrical Engineering, Institute of Power Electronics, Zhejiang University, Hangzhou 310027, China
3 Department of Computer Science and Information, College of Science in Zulfi, Majmaah University, Al-Majmaah 11952, Saudi Arabia
4 Department of Computer Science, College of Computer in Al-Lith, Umm Al-Qura University, Makkah 24382, Saudi Arabia
5 Department of Computer Science, GC Women University, Sialkot 51310, Pakistan
6 College of Computer Science, Zhejiang University, Hangzhou 310027, China
* Correspondence: madiha@zju.edu.cn (M.B.); chenwq@zju.edu.cn (W.C.)

Abstract: In this study, the natural frequencies and roots (Eigenvalues) of the transcendental equation in a cantilever steel beam for transverse vibration with clamped free (CF) boundary conditions are estimated using a long short-term memory-recurrent neural network (LSTM-RNN) approach. The finite element method (FEM) package ANSYS is used for dynamic analysis and, with the aid of simulated results, the Euler–Bernoulli beam theory is adopted for the generation of sample datasets. Then, a deep neural network (DNN)-based LSTM-RNN technique is implemented to approximate the roots of the transcendental equation. Datasets are mainly based on the cantilever beam geometry characteristics used for training and testing the proposed LSTM-RNN network. Furthermore, an algorithm using MATLAB platform for numerical solutions is used to cross-validate the dataset results. The network performance is evaluated using the mean square error (MSE) and mean absolute error (MAE). Finally, the numerical and simulated results are compared using the LSTM-RNN methodology to demonstrate the network validity.

Keywords: clamped free; finite element method; transcendental equation; roots (Eigen values); long short-term memory; recurrent neural network

1. Introduction

Many engineering problems are approached and analyzed using mathematical models developed based on the fundamental principles of engineering. Based on an analysis of the response of the system to various operating loads, numerous systems with applications in mechanical and civil engineering are designed structurally. The technique of conducting a structural dynamic analysis involves solving the governing equations of motion to determine how a system will respond to transient loads, such as the deformation of the system over time and its natural frequencies. The vibrations among engineering structures are amongst their most fundamental characteristics. There are infinite vibrational frequencies and mode forms for every structure in nature [1–3].

Approximate and exact solution methods are used to evaluate natural frequencies. Furthermore, differential equations are applied to these methods to calculate the structural dynamic behavior [4,5]. However, due to the interdependence of these differential equations, numerous factors are encountered while solving them [6,7]. Hence, it is essential to

solve the vibration-induced engineering problems for natural frequencies and mode forms to analyze the vibration of structures [8–13].

Similarly, the literature mentioned in this paragraph provides an analysis of beams with free vibration. For free vibrations with a large amplitude uniform beam, Gupta et al. applied a simplified finite element model [14]. Ramtekkar et al. used a varied finite element model to perform a free vibration study on delaminated beams [15]. Vidal et al. used transverse normal stress and sinus finite elements to study the vibration of multilayered beams [16]. Hong et al. performed an experimental analysis on the transverse vibration of clamped-pinned-free beam with mass at the free end to find the transcendental equation roots of the beam [17].

Although the methodologies mentioned above have been applied to the problems of structural analysis, design and optimization using conventional approaches involve complexity and time-consuming processes. Thus, during the past few decades, soft computing techniques have been widely used in various scientific and engineering fields, particularly in the study of vibration problems in engineering structures. Moreover, such approaches make it easier to perform a vibration analysis of complicated structural systems. Machine learning (ML), artificial neural networks (ANN) and evolutionary algorithms are some well-known soft computing methods used in computational mechanics, especially beam applications [18–20]. For instance, Mehdi et al. presented the natural frequency of the beam using ANN and heuristic research [21]. Aktas et al. use an ANN approach for the transcendental equation of longitudinal vibration [22]. Tekin et al. apply an ANN strategy on the nonlinear vibrations of stepped beam [23]. In order to determine the depth of cracks on a cantilever beam, Kazemi et al. used FEM to evaluate three natural frequencies of the cantilever beam and then further applied an ANN technique trained using particle swarm optimization [24].

Although ANNs and evolutionary techniques show promising performance for analyzing and predicting the beam's natural frequencies, the approaches are implemented with few datasets. Furthermore, the prediction performance evaluation is mainly performed for the natural frequencies of the structural beams. Several traditional methods, such as Newton–Raphson, Bisection, Iteration, etc., have been used to find the transcendental equation roots [25]. However, the problems associated with such conventional methods are as follows: (1) Techniques require numerical iterations for each frequency and root values consequently need a longer computational time; (2) convergence is often slow; and (3) the guess interval cannot be used if there are discontinuities. These issues thus limit the applicability of roots findings, especially for a large number of mode shapes and its corresponding root values. On the other hand, deep neural networks such as the long short-term memory recurrent neural network, show superior capability in terms of performance and their extensive dataset-handling capability in predicting the system parameters. Therefore, this study proposes the LSTM-RNN model for approximating the transcendental equation roots (Eigenvalues) for the first time. Hochreiter and Schmidhuber were the first to develop this network model in 1997 [26]. LSTM-RNN deep neural networks are implemented in numerous research topics, including neural computing, estimating transmission quality, time series forecasting, textual and image recognition, etc. [27–31].

In general, LSTM-RNN contains a collection of layers that are connected to the blocks known as memory blocks [32–35]. All the information is stored in these memory blocks, which are connected with the memory cells and three input, output, and forget multiplicative units. For the structural monitoring of cantilever beams, Vashisht et al. use Bayesian and deep learning LSTM and convolutional neural network (CNN) techniques [36]. Rounak et al. use LSTM-RNN neural networks for damage detection of the structure incorporated into the cantilever beam [37]. Bukhsh et al. use LSTM-RNN neural networks to approximate the polynomial roots [38].

The following are the objectives and sequence of this paper: (1) Throughout the analysis, the first ten natural frequencies and corresponding transcendental roots (Eigenvalues) of prismatic cantilever steel beam (with specifications in Table 1) subjected to clamped

free (CF) boundary condition based on the conventional Euler–Bernoulli beam theory are evaluated as an example; (2) datasets for natural frequencies and roots are generated through FEM package ANSYS; (3) roots are then evaluated numerically with the help of MATLAB programming for cross-validation of the generated dataset results; (4) the proposed LSTM-RNN model is constructed to approximate the roots of the transcendental equation for the transverse vibration of the prismatic cantilever beam with CF case; (5) finally, for the validation of transcendental root values, the results are compared with the FEM ANSYS (datasets), MATLAB (numerical) and LSTM-RNN model (predicted) values. Moreover, network outputs are obtained by adjusting the input data and parameters of the neurons and then further comparing these outputs to the predicted analytically obtained results. Finally, a comparative analysis has been performed between ANSYS, numerical analysis and the proposed network model for ten modes of the natural frequencies and their corresponding transcendental root values.

Table 1. Mechanical parameters and properties of the prismatic cantilever beam.

Parameters (Symbol)	Values (Units)
Length (l)	1.0 m
Breadth (b)	0.10 m
Height (h)	0.03 m
Area of Cross Section (A)	0.266 m^2
Moment of Inertia (I)	2.25×10^{-7} m^4
Number of Modes (n)	1~20,000
Young's Modulus (E)	210×10^9 N/m^2
Poisson's Ratio (v)	0.3
Density (ρ)	7850 kg/m^3

The remaining paper is assembled as follows: Section 2 presents the mathematical modelling, Section 3 elaborates on the fundamental concepts behind the LSTM-RNN model, Section 4 compares analytical and experimental results with a brief discussion, and, Section 5 includes several results and directions for future research.

2. Mathematical Modelling of the Problem

A beam without mass systems with commonly used boundary conditions at each end and including spatial derivatives of up to the third order is shown in Figure 1. The boundary conditions with the name at the top and results at the bottom of each case are based on the Euler–Bernoulli beam theory, where w_1 and w_2 are the dimensionless left and right deflections [3]. Similarly, the prime denotes differentiation with respect to the spatial variable x [39].
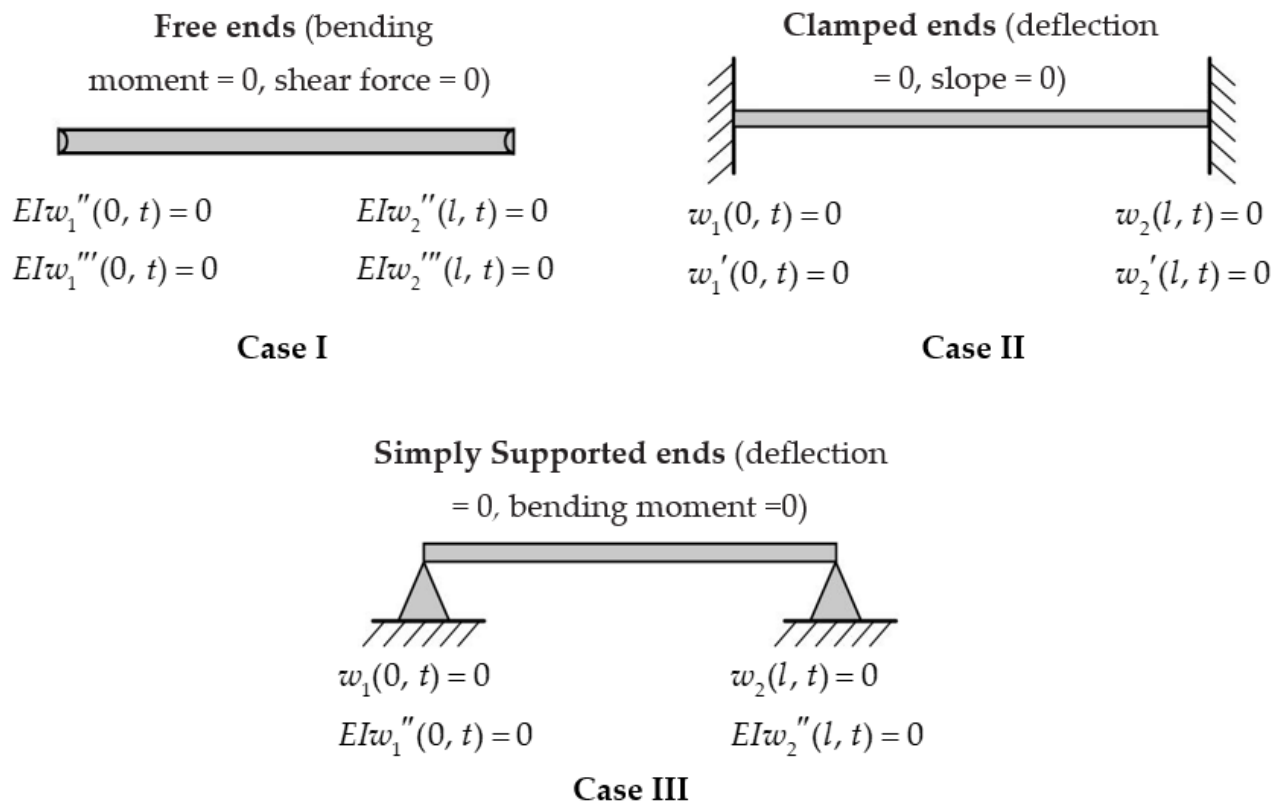
Free ends (bending
moment = 0, shear force = 0)

$EIw_1''(0, t) = 0$ $EIw_2''(l, t) = 0$
$EIw_1'''(0, t) = 0$ $EIw_2'''(l, t) = 0$

Case I

Clamped ends (deflection
= 0, slope = 0)

$w_1(0, t) = 0$ $w_2(l, t) = 0$
$w_1'(0, t) = 0$ $w_2'(l, t) = 0$

Case II

Simply Supported ends (deflection
= 0, bending moment =0)

$w_1(0, t) = 0$ $w_2(l, t) = 0$
$EIw_1''(0, t) = 0$ $EIw_2''(l, t) = 0$

Case III

Figure 1. Different boundary conditions for a beam without mass system.

3. Conventional Analysis

This study presents a combination of case I and II boundary conditions, termed clamped free (CF) boundary conditions, commonly used in prismatic cantilever beam applications and evaluated as examples to approximate the transcendental roots using the proposed methodology. A beam is a slender horizontal structural member that appears in various forms and is used in various artifacts, such as supporting members in high-rise buildings, railways, long-span bridges, flexible satellites, gun barrels, robot arms, airplane wings, balconies and many other areas. Therefore, this section contains mathematical modelling for CF boundary conditions using only a conventional approach based on the work of S. S. Rao [3]. A general 3D view of the prismatic cantilever beam, with beam geometric characteristics such as Young's Modulus E, moment of inertia I, mass density ρ with uniform cross-sectional area A, width W, length L and thickness t, is shown in Figure 2.

The equation of motion for transverse vibration of the prismatic beam with homogenous material parameters and a constant cross-sectional area is derived using the Euler–Bernoulli beam theory [3]:

$$\rho A(x)\frac{\partial^2 \psi(t, x)}{\partial t^2} + \frac{\partial^2}{\partial x^2}\left[EI(x)\frac{\partial^2 \psi(t, x)}{\partial x^2}\right] = 0 \tag{1}$$

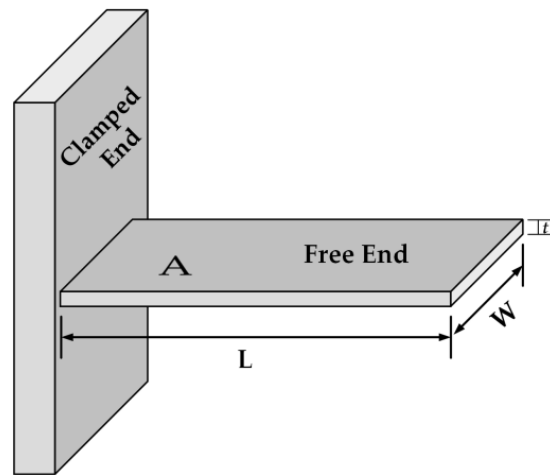where t is time and ψ is the transverse displacement.

Figure 2. Geometry of prismatic cantilever beam.

Equation (1) can be represented in the following simplified form:

$$\frac{\partial^2 \psi}{\partial t^2}(t, x) + \gamma^2 \frac{\partial^4 \psi}{\partial x^4}(t, x) = 0 \tag{2}$$

where

$$\gamma = \sqrt{\frac{IE}{A\rho}} \tag{3}$$

Moreover, Equation (2) is solved by the separation of variables method, defined as:

$$\psi(t, x) = T(t)W(x) \tag{4}$$

Substituting Equation (4) in Equation (2) after some mathematical reconfiguration yields

$$\frac{\gamma^2}{W(x)} \frac{d^4 W(x)}{dx^4} = -\frac{1}{T(t)} \frac{d^2 T(t)}{dt^2} = a = \omega^2 \tag{5}$$

where $a = \omega^2$ can be demonstrated as a positive constant. Equation (5) can be represented as two equations as:

$$\frac{d^4 W(x)}{dx^4} - \beta^4 W(x) = 0 \tag{6}$$

$$\frac{d^2 T(t)}{dt^2} - \omega^2 T(t) = 0 \tag{7}$$

where

$$\beta^4 = \frac{\omega^2}{\gamma^2} = \frac{\rho A \omega^2}{EI} \tag{8}$$

The solution to Equation (7) is given by

$$T(t) = A\cos\omega t + B\sin\omega t \tag{9}$$

Initial conditions can be used to determine the constants A and B. Similarly, the general solution of Equation (6) can be expressed as:

$$W(x) = \quad Z_1(\cosh\beta l + \cos\beta l) + Z_2(\cos\beta l - \cosh\beta l) \\ +Z_3(\sinh\beta l + \sin\beta l) + Z_4(\sin\beta l - \sinh\beta l) \tag{10}$$

The function $W(x)$ is known as the characteristic function or normal mode of the beam, where Z_1, Z_2, Z_3 and Z_4 are the constants and can be determined based on different

boundary conditions. The beam with the CF case is fixed at one end at $x = 0$ and free at the other at $x = l$; hence, transverse deflection and its slope must be zero at $x = 0$, and the bending moment and shear force must also be zero. Consequently, the CF boundary condition is:

$$W(0) = 0 \tag{11}$$

$$\frac{dW}{dx}(0) = 0 \tag{12}$$

$$EI\frac{d^2W}{dx^2}(l) = 0 \tag{13}$$

$$EI\frac{d^3W}{dx^3}(l) = 0 \tag{14}$$

Substituting boundary conditions given in Equations (11)–(14) into Equation (10), respectively, results in:

$$Z_1 = Z_3 = 0 \tag{15}$$

$$Z_2(\cosh\beta l + \cos\beta l) + Z_4(\sinh\beta l + \sin\beta l) = 0 \tag{16}$$

$$Z_2(\sinh\beta l - \sin\beta l) + Z_4(\cosh\beta l + \cos\beta l) = 0 \tag{17}$$

Then, solving and simplifying Equations (16) and (17) gives the transcendental equation:

$$\cosh\beta l \cos\beta l + 1 = 0 \tag{18}$$

Hence, in Equation (18), $\beta_n l$ represents the nth roots (Eigenvalues) of the transcendental or frequency equation, thus providing the natural frequencies (ω_n) of the vibration:

$$\omega_n = (\beta_n l)^2 \sqrt{\frac{IE}{A\rho l^4}}, \; n = 1, 2, \ldots \tag{19}$$

Similarly, the natural frequency (ω_n) of the beam in f_n (Hz) can be found as follows:

$$f_n = \frac{\omega_n}{2\pi} \tag{20}$$

Finally, by manipulating Equations (10), (15) and (16), the corresponding nth mode shape can be derived:

$$W_n(x) = (\cosh\beta_n x + \cos\beta_n x) - \frac{\cosh\beta_n l + \cos\beta_n l}{\sinh\beta_n l + \sin\beta_n l}(\sin\beta_n x - \sinh\beta_n x) \tag{21}$$

4. Long Short-Term Memory (LSTM) Recurrent Neural Network (RNN) Methodology

Deep neural networks (DNNs) with distinct attributes have played an essential role in many applications. LSTM-RNN is a type of DNN that has a solid alternative for gradient vanishing, as well as the regression, classification and prediction of problems because of its capacity to execute tasks requiring nonlinear relationships compared to conventional methods [40]. Similarly, to approximate the roots of the transcendental equation of the prismatic cantilever beam, a multi-layered LSTM-RNN network with hidden layers and hyper-parameters of backpropagation through time is implemented in the proposed network model. An LSTM-RNN network depends on four primary modules, namely a memory block and three logistic gates. Specifically, the memory block is an essential component of the LSTM-RNN model and is used to store the data and this stored data further flows inside the three (read, write, and forget) gates [38].

Moreover, LSTM operations depend on these gates that execute the functions on a linear feature of the network inputs and hidden and prior output states. Although LSTM-RNN can eliminate or add information, which is rigorously controlled by its distinct gates, there is an alternate data maintenance method. Figure 3 is a block diagram of the LSTM-

RNN network which depends on the hidden state h_{t-1} at the previous timestep $t-1$ and h_t is the hidden state at the current timestep t, X_t is the input vector at the current time step t, C_{t-1} is the cell state at the previous timestep $t-1$, and C_t is the cell state at the current timestep t [34].
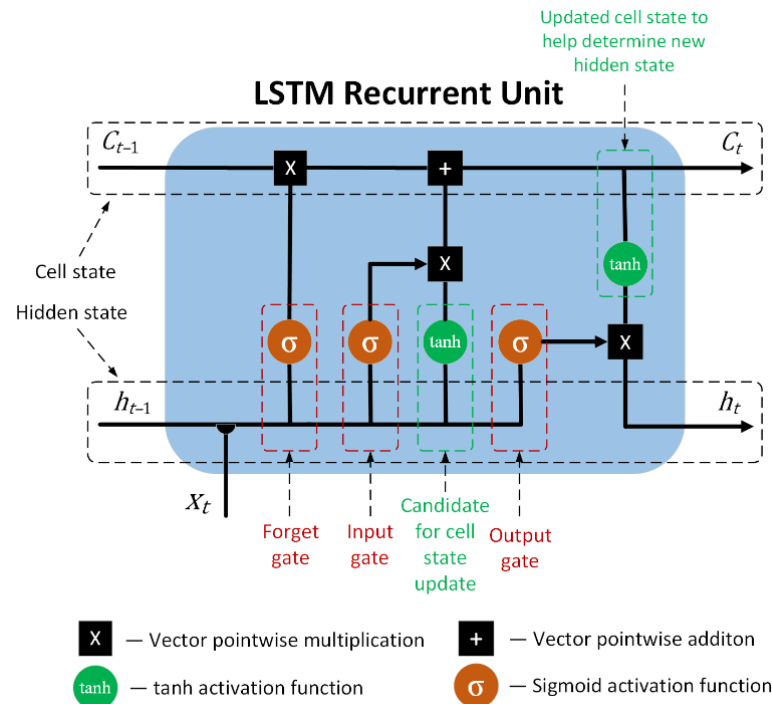

Figure 3. LSTM-RNN network block diagram.

4.1. LSTM-RNN Model Structure for the Problem

Model structures with multiple training hidden layers are intended to approximate the roots (Eigenvalues) of the transcendental equation of the prismatic cantilever beam. The first hidden layer is a 200-neuron LSTM-RNN layer, while the second layer consists of 100 nodes of a completely interconnected opaque layer. Furthermore, for learning parameters, a tangent hyperbolic sigmoid (tanh sigmoid) is adapted as an activation function to be computed and is less liable to saturate zero gradients for the network [41]. Input data for the LSTM-RNN model include features like natural frequency (f_n) and beam geometry characteristics such as a Young's modulus (E), moment of inertia (I), density (ρ), number of modes (n) and cross-sectional area (A). In the meantime, the output layer uses the evaluated roots ($\beta_n l$) as target data output. In addition, an ADAM optimization algorithm which combines the heuristics of both Momentum and RMSProp is adapted to enhance the learning procedure of the network [42]. Similarly, for better accuracy of the predicted values of target data, mean squared error (MSE) and mean absolute error (MAE) functions are applied with value of 0.001 identity regression.

4.2. Datasets Generation for the LSTM-RNN Model

Natural frequencies and the corresponding mode shapes of structures must be obtained to minimize the oscillation in the model design. Theoretical modal analysis is concise for discrete systems but difficult for continuous or multidimensional structure systems. Many engineering problems may be analyzed effectively using finite element programs (FEM). For this purpose, the FEM ANSYS has been widely used to resolve complex engineering problems more efficiently and with less time consumption. Therefore, in this study, datasets are initially generated using ANSYS, which is further used in the LSTM-RNN model to approximate the transcendental equation roots.

For this aim, a total of $n = 20{,}000$, f_n (Hz) datasets of the prismatic beam, having properties as mentioned in Table 1 with CF boundary conditions, are initially generated. Afterward, using Equation (19), roots ($\beta_n l$) of the transcendental equation are numerically computed based on the obtained f_n datasets. Finally, these (f_n, $\beta_n l$) datasets, including beam parameters (A, I, E, ρ, n) as described in the analysis mentioned above, are used as input and output target values for the LSTM-RNN model.

Table 2 illustrates the head of input and output datasets used in the proposed LSTM-RNN model to train and calculate the roots ($\beta_n l$) approximations for $n = 1{\sim}10$ as an example. The latter section shows the associated mode forms of the beam transverse vibration for the first ten natural frequencies.

Table 2. Input and output head datasets for training the LSTM-RNN network for approximating transcendental roots.

	Input Head Datasets		Output Head Datasets
n	f_n (Hz)	$\gamma = \sqrt{\frac{EI}{\rho A}}$	$\beta_n l$
1	25.1	4.756	1.8764
2	156.6	4.756	4.6869
3	436.1	4.756	7.8213
4	847.6	4.756	10.9039
5	1386.9	4.756	13.9479
6	2141.1	4.756	17.3303
7	3005.3	4.756	20.6002
8	3935.6	4.756	23.4959
9	5035.8	4.756	26.4404
10	6421.1	4.756	30.0118
.	.	.	.
.	.	.	.
.	.	.	.
.	.	.	.

4.3. Evaluation Criteria

Empirical results show that the ADAM as an optimizer executes adequately in relation to other stochastic optimization techniques [43]. Furthermore, the theoretical concurrence characteristics of the network model are evaluated using the conventional mean absolute error (MAE) and mean squared error (MSE) functions [38,44]. Similarly, the network learning process is not improved if the function value is too small. As a result, the regret constraints on the convergence rate are equivalent to the results in the field of the optimization method. Therefore, MAE and MSE functions are used to evaluate the adaptability of the LSTM-RNN network model.

$$MSE = \frac{1}{n}\sum_{i=1}^{n}\left(\lambda_N - \hat{\lambda}_N\right)^2 \tag{22}$$

$$MAE = \frac{1}{n}\sum_{n=1}^{n}\left|\lambda_N - \hat{\lambda}_N\right| \tag{23}$$

5. Results and Discussion

In this section, the corresponding mode shapes for the first six natural frequencies of the beam are plotted using ANSYS. Afterward, MATLAB is used to cross-validate the ANSYS-generated datasets for natural frequencies and root parameters. Finally, the proposed LSTM-RNN methodology is implemented to approximate the roots of the transcendental equation.

5.1. FEM ANSYS Simulation

The generated datasets for f_n through ANSYS are tabulated in Table 1. Its corresponding modes shapes for the first six natural frequencies, i.e., $n = 1\sim6$, as an example, are shown below. A 3D model of the bar is made first, and an FE model is subsequently generated. The second step involves applying the CF boundary condition and defining analysis choices, as illustrated in Figure 4. Later, as shown in Figure 5, the first six natural frequencies and related modes (n) for the cantilever beam transverse vibration are established.
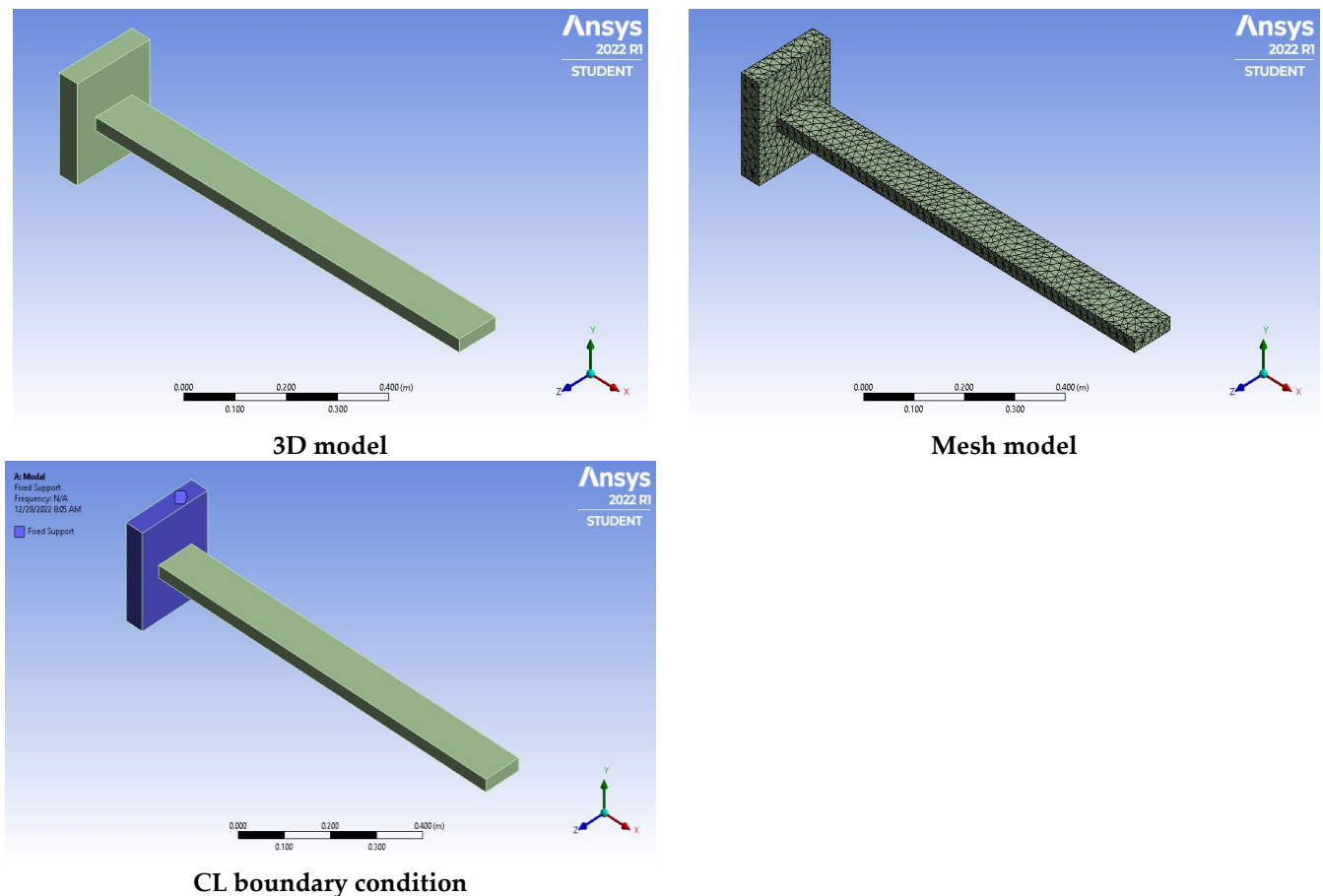

3D model

Mesh model

CL boundary condition

Figure 4. Defining analysis choices for cantilever prismatic beam.

5.2. MATLAB Simulation Analysis

This section aims to cross-validate the accuracy of the ANSYS-generated datasets and numerically computed natural frequency (f_n) and root ($\beta_n l$) values. Although the trigonometric frequency equation is derived analytically in section II, where the values of the root need to be evaluated initially to find the values of natural frequencies (f_n), the development of an algorithm to solve the frequency equations based on a trial-and-error method is proposed. The objective was to find out the roots of the transcendental equation numerically with the help of the programming environment offered in MATLAB.

For this purpose, an approximate estimation of the lower and upper limits for an interval comprising the first few roots, i.e., natural frequencies, can be obtained by visualizing the frequency equation. The roots can then be identified using an incremental search strategy. The frequency equation can then be solved and the algorithm is derived based on the change of sign of a function in the vicinity of a possible root. Finally, frequency Equation (19) is utilized in the MATLAB code containing the root values and the beam properties mentioned in Table 1; f_n in Hz and rad/se are calculated. Moreover, root values

are utilized for the corresponding theoretical mode shapes for the first six modes based on Equation (21), as plotted in Figure 6.
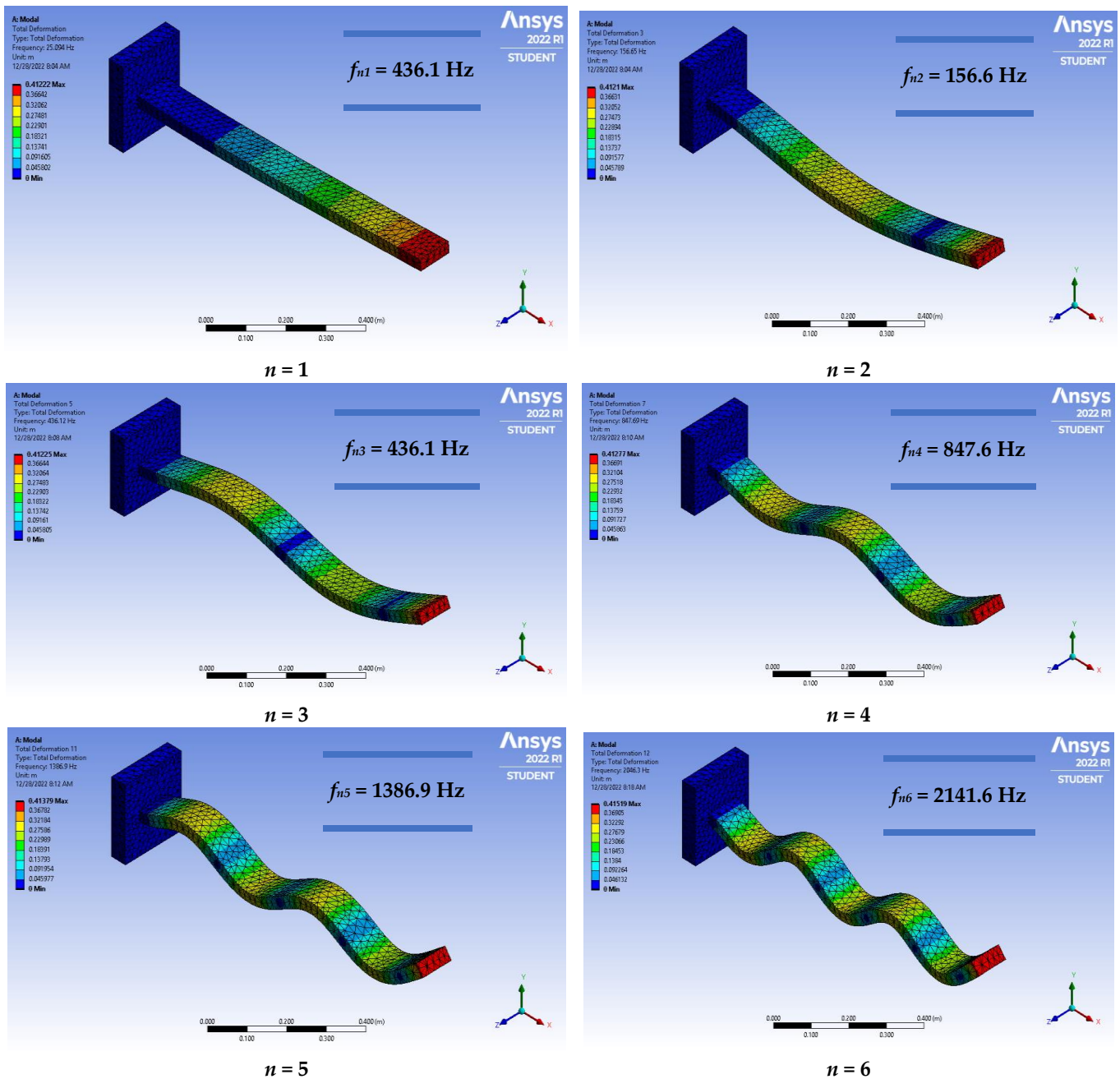

Figure 5. First six mode shapes (*n* = 1~6) of transverse vibration of a cantilever beam.

Calculated based on the technique mentioned above, the first ten f_n and $\beta_n l$ values of the prismatic beam are mentioned in Table 3. The results show that the natural frequency (f_n) and root ($\beta_n l$) values are consistent with ANSYS datasets, thereby cross-validating the results of the numerical approach and generated dataset. In fact, for evaluating the proposed model performance, valid datasets are essential for testing and training the model. Numerical results for roots ($\beta_n l$) are also valid based on the theoretical values of the transverse vibration of the CF beam case mentioned in [3].
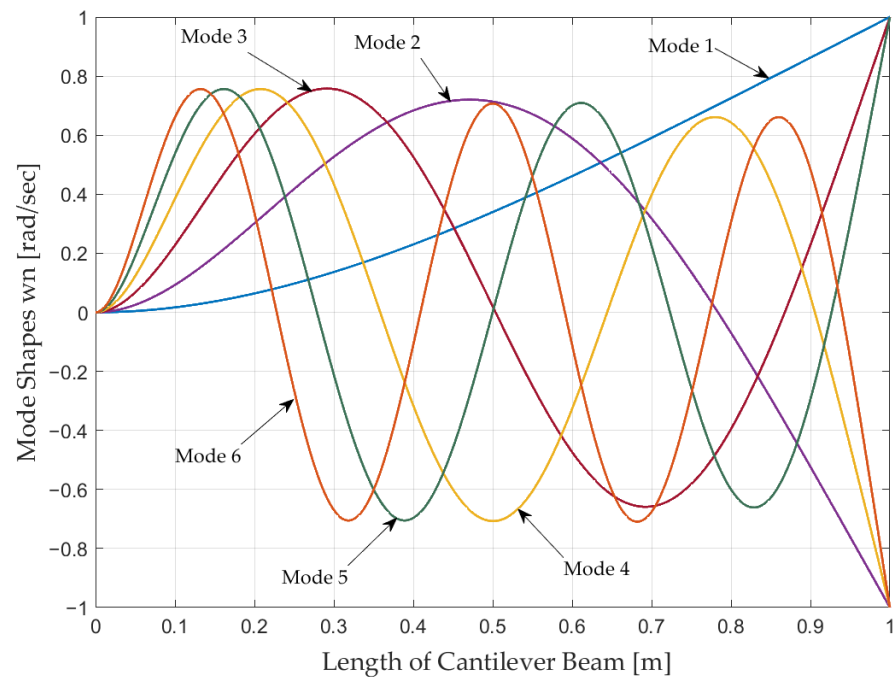
Figure 6. Theoretical mode shapes for first six natural frequencies of a beam.

Table 3. Numerical results using MATLAB.

Modes (*n*)	$\beta_n l$	Freq (rad/s)	Freq (Hz)
1	1.8751	157.71	25.1
2	4.6941	987.09	157.1
3	7.8548	2763.34	439.8
4	10.9955	5415.47	861.9
5	14.1372	8952.27	1424.8
6	17.2788	13,373.12	2128.4
7	20.4203	18.678×10^3	2.9727×10^3
8	23.5619	24.867×10^3	3.9577×10^3
9	26.7035	31.941×10^3	5.0835×10^3
10	29.8451	39.898×10^3	6.3500×10^3

The generalized percentage (%) absolute error equation used for comparison purposes is presented below:

$$\%error = \left| \frac{X_{nSim} - X_{nNum}}{X_{nNum}} \right| \times 100 \tag{24}$$

where X_{nNum} represents the MATLAB numerical values of f_n and $\beta_n l$ parameters. Similarly, X_{nSim} represents the simulated values of f_n and $\beta_n l$ from the ANSYS and LSTM-RNN model, respectively.

Table 4 presents the comparison results with an absolute % error of the first ten natural frequencies between MATLAB (numerical) and ANSYS (datasets) simulated results. Figure 7 shows the comparison results using graphical analysis. The results overlap between each MATALB numerical analysis and ANSYS datasets, thus justifying the cross validation of the results.

Table 4. Comparison of MATLAB (numerical) and ANSYS results.

f_n (Hz)	f_n (Numerical)	f_n (ANSYS)	% Error
f_1	25.1	25.1	0.00
f_2	157.1	156.6	0.32
f_3	439.8	436.1	0.84
f_4	861.9	847.6	1.46
f_5	1424.8	1403.9	1.59
f_6	2128.4	2141.1	0.60
f_7	2972.7	3005.3	1.10
f_8	3957.7	3935.6	0.56
f_9	5083.5	5035.8	0.94
f_{10}	6350.0	6421.1	1.12
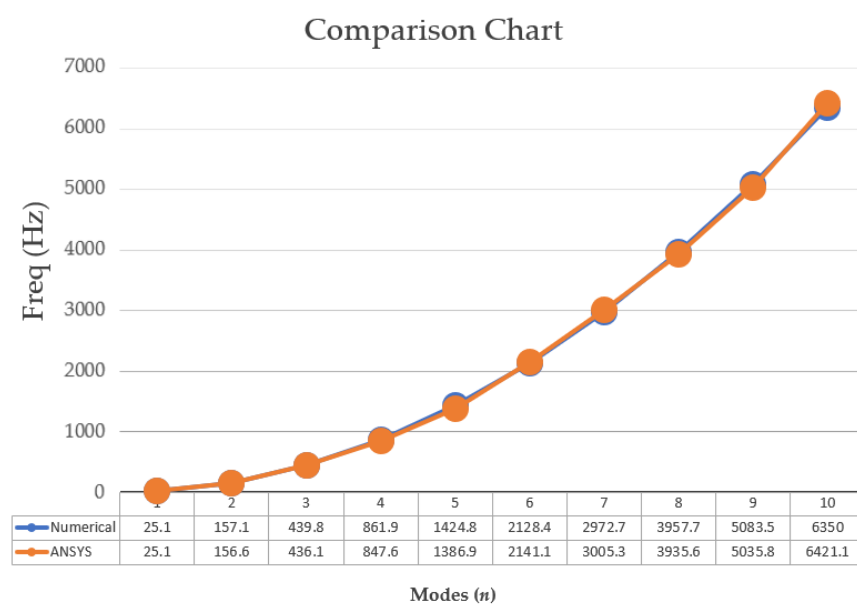
Figure 7. Graphical comparison of f_n results for ten modes.

5.3. LSTM-RNN Model Verification

An approximation of the transcendental equation roots of the prismatic cantilever beam based on the datasets is performed in the proposed LSTM-RNN network. As described above, a total of n = 20,000 datasets have been generated for evaluation purposes, containing input and output data values. The input datasets depend on the parameters of beams and natural frequencies (f_n), while output target datasets contain roots ($\beta_n l$) of the transcendental equation. In this study, 80% of datasets are used in the training set, while the remaining 20% is used for the testing stage.

Figure 8 shows the approximation of transcendental equation roots with 500 epochs. The proposed model performance is examined in terms of both training accuracy and training loss with respect to validation accuracy. Hence, from the results, it has been found that the roots approximation of the prismatic cantilever beam has an accuracy of 96.25% with a means squared error of 0.063% without an overfitting problem.

Similarly, Figure 9 demonstrates the model performance with 1000 epochs. In this case, the training model and validation accuracy is over 98.55% with a mean squared error of 0.042%, respectively.
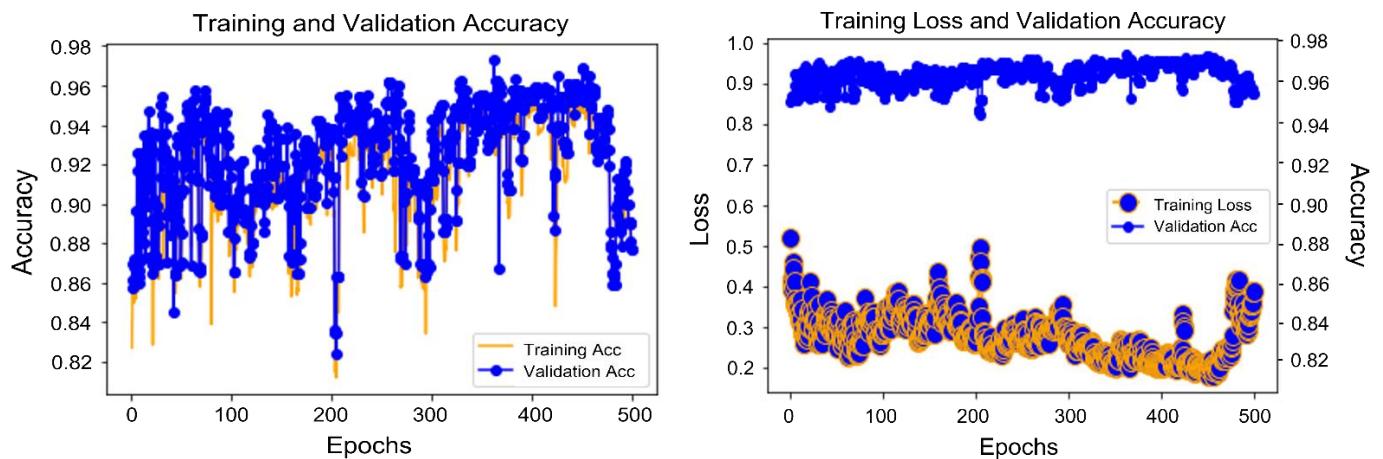
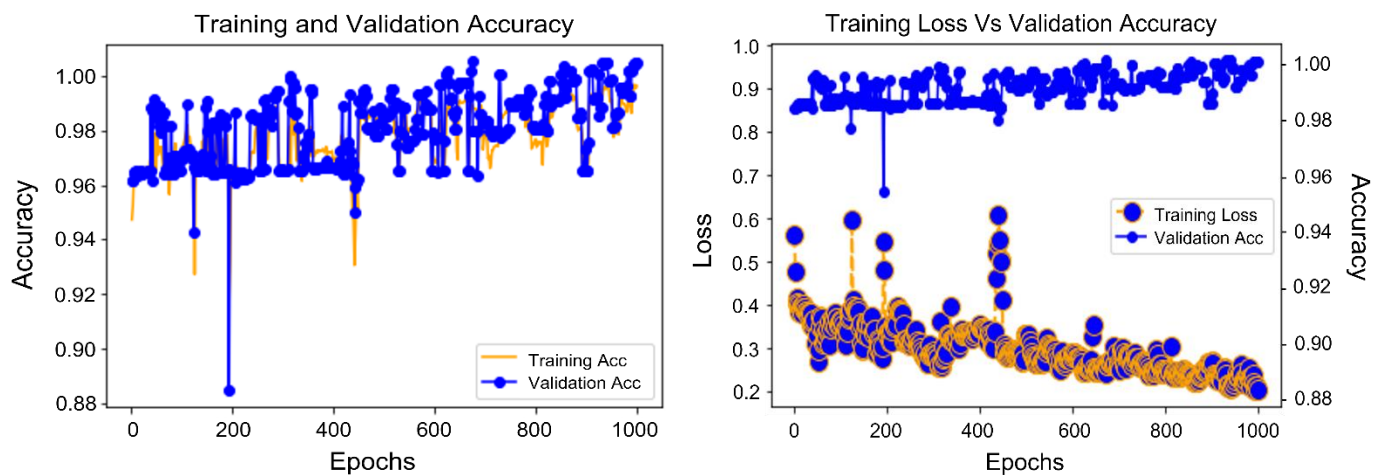**Figure 8.** Validation accuracy vs. training loss and training accuracy results with 500 epochs.

Figure 9. Validation accuracy vs. training loss and training accuracy results with 1000 epochs.

In this study, simulations are performed on Intel Core i-7 with a 1.8 GHz CPU clock and 8 GB RAM. Moreover, the Python programming language version 3.7.4 has been used to implement the LSTM-RNN model.

5.4. Comparative Analysis

In this section, a comparative analysis is performed to show the validity of the proposed methodology. The first ten transcendental equation roots ($\beta_n l$) values, i.e., $n = 1 \sim 10$, have been evaluated as an example. The following is the step-by-step procedure for comparative analysis:

- Frequency (f_n) datasets, based on the prismatic cantilever beam properties mentioned in Table 1, are generated using FEM ANSYS.
- The Euler–Bernoulli Equation (19) is then employed to generate transcendental equation roots ($\beta_n l$).
- For the cross-validation of datasets, f_n and $\beta_n l$ values are calculated numerically using the MATLAB programming platform.
- Based on the input and output target datasets, transcendental roots ($\beta_n l$) values are predicted using the LSTM-RNN model.
- Finally, the transcendental roots (βnl) values are compared among ANSYS (datasets), MATLAB (numerical) and the proposed LSTM-RNN model.

The predicted $\beta_n l$ parameter values based on the LSTM-RNN model are tabulated in Table 5 with a comparative analysis in terms of absolute % error. The $\beta_n l$ results are obtained based on 98.55% accuracy, described in the analysis mentioned above.

Table 5. Comparative analysis of the transcendental roots ($\beta_n l$).

Modes (n)	$\beta_n l$ (Numerical)	$\beta_n l$ (ANSYS)	% Error	$\beta_n l$ (Numerical)	$\beta_n l$ (LSTM-RNN)	% Error	$\beta_n l$ (ANSYS)	$\beta_n l$ (LSTM-RNN)	% Error
1	1.8751	1.8764	0.07	1.8751	1.8505	1.31	1.8764	1.8505	1.38
2	4.6941	4.6869	0.15	4.6941	4.6265	1.44	4.6869	4.6265	1.29
3	7.8548	7.8213	0.43	7.8548	7.7406	1.45	7.8213	7.7406	1.03
4	10.9955	10.9039	0.83	10.9955	10.8565	1.26	10.9039	10.8565	0.43
5	14.1372	13.9479	1.31	14.1372	13.9674	1.20	13.9479	13.9674	0.14
6	17.2788	17.3303	0.30	17.2788	17.3113	0.19	17.3303	17.3113	0.11
7	20.4203	20.6002	0.88	20.4203	20.4141	0.47	20.6002	20.4141	0.85
8	23.5619	23.4959	0.28	23.5619	23.3825	0.34	23.4959	23.3825	0.48
9	26.7035	26.4404	0.99	26.7035	26.6837	0.82	26.4404	26.6837	0.92
10	29.8451	30.0118	0.56	29.8451	29.9538	0.36	30.0118	29.9538	0.19

Table 5 shows that % errors are minimal when a comparison is made between analytical and ANSYS results. The lowest and highest % errors for $\beta_n l$ are 0.07% and 1.31% for $n = 1$ and 5, respectively. On the other hand, compared with analytical and ANSYS $\beta_n l$ results, the proposed LSTM-RNN methodology shows a slightly higher % error, but the highest error is still less than 1.5%.

In fact, it is a more complex and time-consuming process to find a large number of transcendental roots for different beam modes (n) through conventional or analytical methodologies. At the same time, the proposed LSTM-RNN methodology based on ANSYS datasets provides an efficient and simple approach for approximating the roots of the transcendental equation. From the results, it is also concluded that the model accuracy can be further improved by increasing (1) the number of epochs and (2) input and output datasets but at the cost of an increased execution time and a higher demand of system resources.

6. Conclusions

In this study, the root (Eigenvalues) of the transcendental equation of the prismatic steel beams under the clamped free boundary condition are approximated through the proposed LSTM-RNN network. The conclusion of the paper is summarized below:

1. Based on the beam parameters and boundary conditions, natural frequencies (f_n) datasets are initially generated using the finite element method (FEM) ANSYS software. Then, using the fundamental Euler–Bernoulli theory, transcendental root ($\beta_n l$) datasets are produced for implementation in the LSTM-RNN model.
2. An algorithm has been developed to cross-validate the datasets which uses the MATLAB programming platform to find the roots and natural frequencies numerically. The $\beta_n l$ parameter results show consistency with conventional theoretical values. Moreover, the modes shapes for the first six natural frequencies, as an example, have been plotted using ANSYS and MATLAB simulation software.
3. Finally, a comparative analysis between ANSYS (datasets), MATLAB (numerical) and the proposed LSTM-RNN methodology has been performed in terms of percentage (%) MAE and MSE. Although the result shows that the % error is slightly higher than the numerical solution, the performance can be improved by increasing the number of datasets and system resources.
4. The proposed LSTM-RNN method aims to develop an alternative way to find the roots of transcendental or frequency equation based on datasets and beam parameters,

thereby avoiding complexity and time loss in evaluating the beam system with a large number of transverse modes *n*.

In future research, we will consider the case of finding the roots for the transcendental equation under different beam characteristics and with different boundary conditions.

Institutional Review Board Statement: Not applicable.

Informed Consent Statement: Not applicable.

Data Availability Statement: Not applicable.

Conflicts of Interest: The authors declare no conflict of interest.

References

1.   Chung, J.; Yoo, H.H. Dynamic analysis of a rotating cantilever beam by using the finite element method. *J. Sound Vib.* **2002**, *249*, 147–164. [CrossRef]
2.   Jaworski, J.W.; Dowell, E.H. Free vibration of a cantilevered beam with multiple steps: Comparison of several theoretical methods with experiment. *J. Sound Vib.* **2008**, *312*, 713–725. [CrossRef]
3.   Rao, S.S. *Vibration of Continuous Systems*, 3rd ed.; John Wiley & Sons, Inc.: Hoboken, NJ, USA, 2007; ISBN 0471771716.
4.   Sedighi, H.M.; Shirazi, K.H. A new approach to analytical solution of cantilever beam vibration with nonlinear boundary condition. *J. Comput. Nonlinear Dyn.* **2012**, *7*, 034502. [CrossRef]
5.   Wang, C.Y.; Wang, C.M. *Structural Vibration: Exact Solutions for Strings, Membranes, Beams, and Plates*, 1st ed.; CRC Press: Boca Raton, FL, USA, 2016; ISBN 1466576841.
6.   Bahrami, M.N.; Arani, M.K.; Saleh, N.R. Modified wave approach for calculation of natural frequencies and mode shapes in arbitrary non-uniform beams. *Sci. Iran.* **2011**, *18*, 1088–1094. [CrossRef]
7.   Sedighi, H.M.; Shirazi, K.H.; Noghrehabadi, A. Application of recent powerful analytical approaches on the non-linear vibration of cantilever beams. *Int. J. Nonlinear Sci. Numer. Simul.* **2012**, *13*, 487–494. [CrossRef]
8.   Romaszko, M.; Sapiński, B.; Sioma, A. Forced vibrations analysis of a cantilever beam using the vision method. *J. Theor. Appl. Mech.* **2015**, *53*, 243–254. [CrossRef]
9.   Civalek, Ö.; Gürses, M. Free vibration analysis of rotating cylindrical shells using discrete singular convolution technique. *Int. J. Press. Vessel. Pip.* **2009**, *86*, 677–683. [CrossRef]
10. Banerjee, J.R. Review of the dynamic stiffness method for free-vibration analysis of beams. *Transp. Saf. Environ.* **2019**, *1*, 106–116. [CrossRef]
11. Avcar, M. Free Vibration Analysis of Beams Considering Different Geometric Characteristics and Boundary Conditions. *Int. J. Mech. Appl.* **2014**, *4*, 94–100. [CrossRef]
12. Prokić, A.; Bešević, M.; Lukić, D. A numerical method for free vibration analysis of beams. *Lat. Am. J. Solids Struct.* **2014**, *11*, 1432–1444. [CrossRef]
13. Yesilce, Y. Differential transform method and numerical assembly technique for free vibration analysis of the axial-loaded Timoshenko multiple-step beam carrying a number of intermediate lumped masses and rotary inertias. *Struct. Eng. Mech.* **2015**, *53*, 537–573. [CrossRef]
14. Gupta, R.; Babu, G.J.; Janardhan, G.R.; Rao, G.V. Relatively simple finite element formulation for the large amplitude free vibrations of uniform beams. *Finite Elem. Anal. Des.* **2009**, *45*, 624–631. [CrossRef]
15. Ramtekkar, G.S. Free vibration analysis of delaminated beams using mixed finite element model. *J. Sound Vib.* **2009**, *328*, 428–440. [CrossRef]
16. Vidal, P.; Polit, O. Vibration of multilayered beams using sinus finite elements with transverse normal stress. *Compos. Struct.* **2010**, *92*, 1524–1534. [CrossRef]
17. Hong, J.; Dodson, J.; Laflamme, S.; Downey, A. Transverse vibration of clamped-pinned-free beam with mass at free end. *Appl. Sci.* **2019**, *9*, 2996. [CrossRef]
18. Burnwal, A.P. On soft computing techniques in various areas. *Comput. Sci. Inf. Technol.* **2013**, *3*, 59–68. [CrossRef]

19. Vadyala, S.R.; Betgeri, S.N.; Matthews, J.C.; Matthews, E. A Review of Physics-Based Machine Learning in Civil Engineering. *Results Eng.* **2022**, *13*, 100316. [CrossRef]
20. Gates, R.; Choi, M.; Biswas, S.K.; Helferty, J.J. Stabilization of flexible structures using artificial neural networks. In Proceedings of the International Joint Conference on Neural Networks, Nagoya, Japan, 25–29 October 1993.
21. Nikoo, M.; Hadzima-Nyarko, M.; Nyarko, E.K.; Nikoo, M. Determining the Natural Frequency of Cantilever Beams Using ANN and Heuristic Search. *Appl. Artif. Intell.* **2018**, *32*, 309–334. [CrossRef]
22. AKTAŞ, G.R.; EMUL, A.; ORHAN, S. An Artificial Neural Network (ANN) Approach For Solution Of The Transcendental Equation Of Longitudinal Vibration. *Univ. J. Fac. Eng.* **2019**, *24*, 161–170. [CrossRef]
23. Bağdatli, S.M.; Özkaya, E.; Özyiğit, H.A.; Tekin, A. Non linear vibrations of stepped beam systems using artificial neural networks. *Struct. Eng. Mech.* **2009**, *33*, 15–30. [CrossRef]
24. Kazemi, M.A.; Nazari, F.; Karimi, M.; Baghalian, S.; Rahbarikahjogh, M.A.; Khodabandelou, A.M. Detection of multiple cracks in beams using particle swarm optimization and artificial neural network. In Proceedings of the 4th International Conference on Modeling, Simulation and Applied Optimization, Kuala Lumpur, Malaysia, 19–21 April 2011.
25. Gupta, R.K. *Numerical Methods: Fundamentals and Applications*, 1st ed.; Cambridge University Press: Cambridge, UK, 2019; ISBN 9781108716000.
26. Hochreiter, S.; Schmidhuber, J. Long Short-Term Memory. *Neural Comput.* **1997**, *9*, 1735–1780. [CrossRef] [PubMed]
27. Aladin, S.; Tran, A.V.S.; Allogba, S.; Tremblay, C. Quality of Transmission Estimation and Short-Term Performance Forecast of Lightpaths. *J. Light. Technol.* **2020**, *38*, 2806–2813. [CrossRef]
28. Ma, J.; Liu, H.; Peng, C.; Qiu, T. Unauthorized Broadcasting Identification: A Deep LSTM Recurrent Learning Approach. *IEEE Trans. Instrum. Meas.* **2020**, *69*, 5981–5983. [CrossRef]
29. Sahoo, B.B.; Jha, R.; Singh, A.; Kumar, D. Long short-term memory (LSTM) recurrent neural network for low-flow hydrological time series forecasting. *Acta Geophys.* **2019**, *67*, 1471–1481. [CrossRef]
30. Gaafar, A.S.; Dahr, J.M.; Hamoud, A.K. Comparative Analysis of Performance of Deep Learning Classification Approach Based on LSTM-RNN for Textual and Image Datasets. *Informatica* **2022**, *46*, 21–28. [CrossRef]
31. Luo, X.; Zhang, D.; Zhu, X. Deep Learning Based Forecasting of Photovoltaic Power Generation by Incorporating Domain Knowledge. *Energy* **2021**, *225*, 120240. [CrossRef]
32. Van Houdt, G.; Mosquera, C.; Nápoles, G. A Review on the Long Short-Term Memory Model. *Artif. Intell. Rev.* **2020**, *53*, 5929–5955. [CrossRef]
33. Shrestha, A.; Mahmood, A. Review of Deep Learning Algorithms and Architectures. *IEEE Access* **2019**, *7*, 53040–53065. [CrossRef]
34. Goodfellow, I.; Bengio, Y.; Courville, A. *Deep Learning*; An MIT Press Book: Cambridge, MA, USA, 2016; ISBN 9780262035613.
35. Chollet, F. *Deep Learning with Python*, 2nd ed.; Manning Publications Co.: Shelter Island, NY, USA, 2021; ISBN 1617296864.
36. Vashisht, R.; Viji, H.; Sundararajan, T.; Mohankumar, D.; Sumitra, S. Structural Health Monitoring of Cantilever Beam, a Case Study—Using Bayesian Neural Network and Deep Learning. *Lect. Notes Mech. Eng.* **2020**, *2*, 749–761. [CrossRef]
37. De, R.; Kundu, A.; Chakraborty, S. Long Short-Term Memory-Based Deep Learning Algorithm for Damage Detection of Structure. In *Recent Advances in Computational and Experimental Mechanics*; Maiti, D., Jana, P., Eds.; Springer: Singapore, 2022; Volume 2, pp. 325–335. [CrossRef]
38. Bukhsh, M.; Ali, M.S.; Ashraf, M.U.; Alsubhi, K.; Chen, W. An Interpretation of Long Short-Term Memory Recurrent Neural Network for Approximating Roots of Polynomials. *IEEE Access* **2022**, *10*, 28194–28205. [CrossRef]
39. Li, W.L. Free vibrations of beams with general boundary conditions. *J. Sound Vib.* **2000**, *237*, 709–725. [CrossRef]
40. Ruder, S. An overview of gradient descent optimization algorithms. *arXiv* **2016**, arXiv:1609.04747.
41. Sengupta, A.; Seal, A.; Panigrahy, C.; Krejcar, O.; Yazidi, A. Edge Information Based Image Fusion Metrics Using Fractional Order Differentiation and Sigmoidal Functions. *IEEE Access* **2020**, *8*, 88385–88398. [CrossRef]
42. Kingma, D.P.; Ba, J.L. Adam: A method for stochastic optimization. In Proceedings of the 3rd International Conference on Learning Representations, San Diego, CA, USA, 7–9 May 2015.
43. Marti, K. *Stochastic Optimization Methods*; Springer: Berlin/Heidelberg, Germany, 2005; Volume 2.
44. Wang, W.; Lu, Y. Analysis of the Mean Absolute Error (MAE) and the Root Mean Square Error (RMSE) in Assessing Rounding Model. *IOP Conf. Ser. Mater. Sci. Eng.* **2018**, *324*, 012049. [CrossRef]